

## Rayleigh-Bénard Convection in a Near-Critical Fluid in the Neighborhood of the Stability Threshold

V. I. Polezhaev and E. B. Soboleva

Received July 8, 2004

**Abstract** — Steady-state Rayleigh-Bénard convection in a medium with parameters close to the thermodynamic critical point is simulated within the framework of the complete Navier-Stokes equations with a two-scale representation of the pressure and the Van-der-Waals equation of state. A calibration relation is obtained for a realistic Rayleigh number in a compressible stratified medium. The parameters of the numerical simulation are determined from experimental data for near-critical helium on the basis of the calibration relation. The threshold Rayleigh numbers are found without and with allowance for stratification and a comparison with the experimental and theoretical data is carried out. The effect of compressibility of the near-critical fluid on steady-state convection flows is investigated beyond the stability threshold and the effect of adiabatic compression of the medium is analyzed.

**Keywords:** near-critical fluid, Rayleigh-Bénard convection, simulation, stratification, hydrostatic compressibility, adiabatic compression.

The problem of fluid or gas convection in a plane horizontal layer heated from below (Rayleigh-Bénard problem) is one of the basic hydrodynamic problems studied in hydrodynamic stability and heat transfer theories and has many diverse applications, in particular, in investigating large-scale motions in geo- and astrophysics. Many authors have reviewed this research; we will mention only [1–3], published in the last decade, which contain the complete bibliography. The Oberbeck-Boussinesq approximation used for a weakly compressible medium is frequently employed in convection theory. This is entirely justified in many practical cases. In this formulation the convection regime is determined by the Rayleigh number and the onset of motion is determined by the threshold Rayleigh number. Already many investigations have been carried out on the basis of the Oberbeck-Boussinesq model, including both calculations of two- and three-dimensional flows in the neighborhood of the stability threshold of mechanical equilibrium and calculations of transition and turbulent regimes with an exceptionally complex structure [2–5]. The calculations were performed using direct numerical simulation methods.

However, in recent years fluids with parameters in the neighborhood of the thermodynamic critical point (near-critical fluids) which have unusual properties, in particular, high compressibility, have attracted great attention [6]. As the distance from the critical point decreases, the compressibility of these fluids increases and tends to infinity at the critical point. For such systems the Oberbeck-Boussinesq approximation cannot be used, except in certain particular cases, since the stratification effects are already significant even on the laboratory scale.

In a compressible medium without viscosity and heat conduction the stable state is maintained due to the density stratification associated with hydrostatic compressibility. The onset of convection is determined by the limiting temperature gradient which was first found by Schwarzschild and is known in geo- and astrophysical literature as the adiabatic temperature gradient. A general form of the expression for the adiabatic temperature gradient was given in [7]. However, in order to find the conditions of onset of convection in a near-critical fluid it is necessary to know this quantity in more detail since the physical properties of the medium in the neighborhood of the critical point change substantially. For this purpose in [8] the equations of isentropic equilibrium were solved and the adiabatic temperature gradient as a function of the height in

a Van-der-Waals gas was found. A compressible medium with dissipation was considered in [9], where a modified Rayleigh number, which includes the difference between the real and adiabatic temperature gradients instead of the real temperature gradient, was proposed as the criterion of onset of the motion.

In the first numerical investigations of Rayleigh-Bénard convection in a compressible perfect gas carried out on the basis of the Navier-Stokes equations the condition of loss of stability was determined from the supercritical state as the Rayleigh number decreases until the regime of heat transfer via heat conduction is attained [10]. In this case the mutual influence of the Rayleigh and Schwarzschild criteria on the onset and development of convection was taken into account and it was found that the threshold Rayleigh number calculated without regard for stratification increases with the compressibility of the medium. The threshold value of the modified Rayleigh number, which includes the difference between the real and adiabatic temperature gradients [9] is almost independent of the hydrostatic compressibility [11].

In [12] consideration of the conditions of loss of stability of mechanical equilibrium in a near-critical fluid was begun within the framework of a simplified model; recently, in [13] a fuller analysis of the onset of convection in a medium with the Van-der-Waals equation of state in the neighborhood of the critical point was carried out and a criterion of onset of motion similar to that of [12] was found. As for a perfect gas, the modified Rayleigh number, whose form in [13] coincides with that given in [9], is the determining parameter and its threshold value for a layer between two rigid boundaries is constant and equal to 1708, i.e., to the threshold value of the Rayleigh number in the Oberbeck-Boussinesq approximation.

The theoretical representations so far accumulated make it possible a close approach to the analysis and interpretation of experiments on Rayleigh-Bénard convection in near-critical media [14–16]. Extensive data on heat transfer in helium from the onset of convection to initial turbulence presented in [16] initiated studies [17–20] on numerical simulation under experimental conditions. In these studies the unsteady phenomena developing in the interaction between convection and a type of heating called the piston effect, in which the medium is heated due to adiabatic compression, were mainly investigated [21]. In experiments [16] the threshold Rayleigh number was also found and the stratification effects due to hydrodynamic compressibility were investigated. Attempts to compare the numerical results for the stability threshold were made in [22], where, however, the role of stratification was unimportant since the conditions were considered at a large distance from the critical point.

As compared with [22], in the present study we have carried out a fuller numerical simulation of steady-state Rayleigh-Bénard convection in helium with near-critical characteristics in the neighborhood of the stability threshold of mechanical equilibrium under the experimental conditions of [16]. The complete Navier-Stokes equations with a two-scale representation of the pressure and the Van-der-Waals equation of state are solved. A calibration relation for the Rayleigh number extended to convection flows with allowance for stratification is introduced and used for calculating the simulation parameters. The threshold Rayleigh numbers are determined for various distances from the critical point. The effect of stratification on onset of motion is analyzed and, following the general approach [10, 11], the hydrodynamic compressibility effects in steady-state Van-der-Waals gas flows are studied.

## 1. MATHEMATICAL DESCRIPTION OF A NEAR-CRITICAL FLUID AND CALIBRATION RELATIONS

We will describe the dynamics of the near-critical fluid within the framework of the hydrodynamic model including the complete Navier-Stokes equations with a two-scale representation of the pressure and a two-parameter equation of state of an imperfect gas. In dimensionless form the input system of equations can be written as follows [23]:

$$\frac{\partial \rho}{\partial t} + \nabla(\rho \mathbf{U}) = 0 \quad (1.1)$$

$$\rho \frac{\partial \mathbf{U}}{\partial t} + \rho(\mathbf{U} \nabla) \mathbf{U} = -\nabla p + \frac{1}{\text{Re}} \left( 2\nabla(\eta \dot{\mathbf{D}}) - \nabla \left( \frac{2}{3} \eta - \zeta \right) \nabla \mathbf{U} \right) + \frac{\text{Ra}}{\text{Pr} \Theta \text{Re}^2} \rho \mathbf{g} \quad (1.2)$$

$$\rho \frac{\partial T}{\partial t} + \rho(\mathbf{U}\nabla)T = -(\gamma_0 - 1)T \left( \frac{\partial P}{\partial T} \right)_\rho \nabla\mathbf{U} + \frac{\gamma_0}{\text{RePr}} \nabla(\lambda \nabla T) + \frac{\gamma_0(\gamma_0 - 1)\text{M}^2}{\text{Re}} \left( 2\eta \mathbf{D}^2 - \nabla \left( \frac{2}{3}\eta - \zeta \right) (\nabla\mathbf{U})^2 \right) \quad (1.3)$$

$$P = P(\rho, T), \quad P = \langle P \rangle + \gamma_0 \text{M}^2 p, \quad \int_V p dv = 0 \quad (1.4)$$

Here,  $\rho$ ,  $\mathbf{U}$ ,  $\mathbf{D}$ , and  $T$  are the density, the velocity, the strain rate tensor, and the gas temperature;  $P$ ,  $\langle P \rangle$ , and  $p$  are the total, average, and dynamic pressures,  $\mathbf{g}$  is the gravity force acceleration;  $\eta$ ,  $\zeta$ , and  $\lambda$  are the dynamic and second viscosities and the thermal conductivity,  $dv$  is a volume element of the domain, and  $V$  is the total volume. The characteristic scales are as follows:  $l'$ ,  $U'$ ,  $l'/U'$ ,  $U'/l'$  ( $l'$  is the length),  $\rho'_c$ ,  $T'_c$  (subscript  $c$  denotes the quantities at the critical point),  $B'\rho'_c T'_c$  for  $P$ ,  $\langle P \rangle$ ,  $\rho'_c U_c'^2$  for  $p$ ,  $\lambda'_0$ ,  $\eta'_0$ ,  $c'_{v0}$  (subscript “0” denotes the parameters of a perfect gas and  $c'_v$  is the specific heat at constant pressure), and the Earth’s gravity force acceleration  $g'$ . Dimensional quantities are denoted by primes and the dimensionless ones have no prime.

Splitting of the total pressure into two components used earlier in the perfect gas model [24] makes it possible effectively to simulate both the acoustic and slow (convective) processes; more detailed explanations are given in [23].

System (1.1)–(1.4) contains the following dimensionless parameters:

$$\begin{aligned} \text{Re} &= \frac{\rho'_c U' l'}{\eta'_0}, & \text{Ra} &= \frac{\Theta' g' l'^3 \rho'^2 (c'_{v0} + B')}{T'_c \lambda'_0 \eta'_0}, & \text{Pr} &= \frac{(c'_{v0} + B') \eta'_0}{\lambda'_0} \\ \Theta &= \frac{\Theta'}{T'_c}, & \gamma_0 &= 1 + \frac{B'}{c'_{v0}}, & \text{M} &= \frac{U'}{\sqrt{\gamma_0 B' T'_c}} \end{aligned} \quad (1.5)$$

which represent the Reynolds, Rayleigh, and Prandtl numbers, the characteristic temperature difference, the specific heat ratio, and the Mach number, respectively.

The medium is stratified; under the hydrostatic equilibrium conditions the density and total pressure  $\rho$  and  $P$  are assumed to vary linearly

$$\rho = \rho_b \left( 1 + \left( \frac{\partial \rho_b}{\partial p_b} \right)_T \varepsilon_g \mathbf{g}(\mathbf{r} - \mathbf{r}_b) \right), \quad P = p_b + \rho_b \varepsilon_g \mathbf{g}(\mathbf{r} - \mathbf{r}_b), \quad \varepsilon_g = \frac{\gamma_0 \text{M}^2 \text{Ra}}{\text{Pr} \Theta \text{Re}^2} \quad (1.6)$$

Here,  $\varepsilon_g$  is the hydrostatic compressibility parameter. On the boundary at a point with the radius-vector  $\mathbf{r}_b$  the quantities are denoted by the subscript “ $b$ ”. For a very close approach to the critical point the density and pressure distributions over the height are more complex; however, under the conditions in question approximation (1.6) can be used.

In the neighborhood of the critical point the thermal conductivity  $\lambda$  increases asymptotically:  $\lambda = 1 + \Lambda \varepsilon^{-\psi}$ , where  $\varepsilon = (T' - T'_c)/T'_c$  is the temperature parameter characterizing the proximity to the critical point and the viscosities are constant:  $\eta = \text{const}$  and  $\zeta = 0$ . In order to define the model system of equations uniquely it is necessary to give concrete expression to the equation of state (1.4). We will use the Van-der-Waals equation of state

$$P = \frac{\rho T}{1 - b\rho} - a\rho^2, \quad a = \frac{9}{8}, \quad b = \frac{1}{3} \quad (1.7)$$

It is a feature of the dynamics of near-critical fluids that the model numbers Ra and Pr (1.5) which enter into the main system of equations are constructed on the basis of characteristics of the medium far away from the critical point and in themselves do not describe the variations of the physical properties in the neighborhood of the critical point. However, as the distance from the critical point decreases, the true

values of the Rayleigh and Prandtl numbers tend to infinity; therefore, it has been proposed to consider modified dimensionless numbers, called real in [25], which take into account the features of the behavior of thermodynamic quantities in the critical neighborhood. For flows “insensitive” to stratification an expression for the real Rayleigh number  $Ra_r$  denoted by the subscript “ $r$ ” was obtained in [25]; in the case of stratified media this expression need to be corrected.

The convection of a near-critical fluid in the presence of stratification can be characterized by the modified Rayleigh number  $Ra_r^s$  [13]:

$$Ra_r^s = \left( \frac{\partial \Theta'}{\partial y'} - \left( \frac{\partial \Theta'}{\partial y'} \right)_{ad} \right) \frac{\beta' g' l'^4 \rho'^2 c'_p}{\lambda' h'} \quad (1.8)$$

Instead of the quantity  $\partial \Theta' / \partial y'$  in  $Ra_r$ , expression (1.8) contains the difference between the real temperature gradient in the neighborhood of the heated boundary  $\partial \Theta' / \partial y'$  and the adiabatic temperature gradient  $(\partial \Theta' / \partial y')_{ad}$  and  $c'_p$  is the specific heat at constant pressure. We can readily obtain the relation between  $Ra_r$  and  $Ra_r^s$

$$Ra_r^s = k Ra_r, \quad k = 1 - \frac{(\partial \Theta' / \partial y')_{ad}}{\partial \Theta' / \partial y'} \quad (1.9)$$

We will investigate a neighborhood of the critical isochore (the properties of the fluid depend only on the temperature parameter  $\varepsilon$ ). Under these conditions the expression for  $Ra_r$  characteristic of the medium with a Van-der-Waals equation of state has the form [25]:

$$Ra_r = \frac{2}{3} \varepsilon^{-1} \left( \frac{1}{\gamma_0} + \frac{\gamma_0 - 1}{\gamma_0} \frac{1 + \varepsilon}{\varepsilon} \right) \frac{1}{\lambda} Ra \quad (1.10)$$

We will find the coefficient  $k$ . Following [7], we define the adiabatic temperature gradient by the relation

$$\left( \frac{\partial \Theta'}{\partial y'} \right)_{ad} = \frac{g' \beta' T'}{c'_p} \quad (1.11)$$

The coefficients  $\beta'$  and  $c'_p$  depend on the parameters of the medium in accordance with the following expressions [26]:

$$\beta' = -\frac{1}{\rho'} \left( \frac{\partial \rho'}{\partial T'} \right)_{P'}, \quad c'_p = c'_v + \frac{T'}{\rho'^2} \left( \frac{\partial P'}{\partial T'} \right)_{\rho'}^2 \left( \frac{\partial \rho'}{\partial P'} \right)_{T'} \quad (1.12)$$

which diverge asymptotically at the critical point since  $(\partial \rho' / \partial T')_{P'} \rightarrow \infty$  and  $(\partial \rho' / \partial T')_{T'} \rightarrow \infty$ . Using the Van-der-Waals equation of state, we can obtain the following expression for the adiabatic temperature gradient:

$$\left( \frac{\partial \Theta'}{\partial y'} \right)_{ad} = \frac{2g'}{3B' \varepsilon + (1 + \varepsilon)(\gamma_0 - 1)} \quad (1.13)$$

Estimating the real temperature gradient as the ratio of the temperature difference on the boundary of the domain and the distance between the boundaries  $\partial \Theta' / \partial y' = \Theta' / l'$ , we obtain the dependence

$\varepsilon$	$\lambda$	$c_p$	$\beta$	$Ra_e/\Theta$	$Pr_e$
$5.00 \cdot 10^{-4}$	2.99	$2.05 \cdot 10^4$	$5.99 \cdot 10^3$	$2.28 \cdot 10^{14}$	586
$1.00 \cdot 10^{-3}$	2.32	$9.03 \cdot 10^4$	$2.64 \cdot 10^3$	$5.74 \cdot 10^{13}$	328
$2.00 \cdot 10^{-3}$	1.86	$3.97 \cdot 10^4$	$1.16 \cdot 10^3$	$1.38 \cdot 10^{13}$	177
$5.00 \cdot 10^{-3}$	1.47	$1.35 \cdot 10^4$	$3.91 \cdot 10^2$	$2.00 \cdot 10^{12}$	74.8
$9.00 \cdot 10^{-3}$	1.32	$6.86 \cdot 10^3$	$1.96 \cdot 10^2$	$5.68 \cdot 10^{11}$	41.9
$1.00 \cdot 10^{-2}$	1.30	$6.08 \cdot 10^3$	$1.73 \cdot 10^2$	$4.55 \cdot 10^{11}$	37.7
$2.00 \cdot 10^{-2}$	1.18	$2.78 \cdot 10^3$	$7.68 \cdot 10^1$	$1.01 \cdot 10^{11}$	18.7
$3.00 \cdot 10^{-2}$	1.13	$1.78 \cdot 10^3$	$4.82 \cdot 10^1$	$4.22 \cdot 10^{10}$	12.4
$4.00 \cdot 10^{-2}$	1.10	$1.31 \cdot 10^3$	$3.45 \cdot 10^1$	$2.21 \cdot 10^{10}$	9.28
$5.00 \cdot 10^{-2}$	1.09	$1.03 \cdot 10^3$	$2.67 \cdot 10^1$	$1.41 \cdot 10^{10}$	7.43
$6.00 \cdot 10^{-2}$	1.08	$8.56 \cdot 10^2$	$2.16 \cdot 10^1$	$9.56 \cdot 10^9$	6.22
$7.00 \cdot 10^{-2}$	1.07	$7.34 \cdot 10^2$	$1.82 \cdot 10^1$	$6.94 \cdot 10^9$	5.36
$8.00 \cdot 10^{-2}$	1.06	$6.41 \cdot 10^2$	$1.55 \cdot 10^1$	$5.21 \cdot 10^9$	4.71
$9.00 \cdot 10^{-2}$	1.06	$5.72 \cdot 10^2$	$1.35 \cdot 10^1$	$4.08 \cdot 10^9$	4.22
$1.00 \cdot 10^{-1}$	1.06	$5.17 \cdot 10^2$	$1.20 \cdot 10^1$	$3.26 \cdot 10^9$	3.83
$1.20 \cdot 10^{-1}$	1.05	$4.36 \cdot 10^2$	9.65	$2.22 \cdot 10^9$	3.25
$1.40 \cdot 10^{-1}$	1.05	$3.80 \cdot 10^2$	8.00	$1.61 \cdot 10^9$	2.84
$1.60 \cdot 10^{-1}$	1.05	$3.37 \cdot 10^2$	6.75	$1.20 \cdot 10^9$	2.53
$1.70 \cdot 10^{-1}$	1.05	$3.19 \cdot 10^2$	6.23	$1.05 \cdot 10^9$	2.41
$1.80 \cdot 10^{-1}$	1.05	$3.04 \cdot 10^2$	5.78	$9.29 \cdot 10^8$	7.07
$2.00 \cdot 10^{-1}$	1.06	$2.78 \cdot 10^2$	5.00	$7.30 \cdot 10^8$	6.48

$$k = 1 - \frac{2\varepsilon_g}{3\Theta} \frac{(1 + \varepsilon)(\gamma_0 - 1)}{\varepsilon + (1 + \varepsilon)(\gamma_0 - 1)} \quad (1.14)$$

In [25] the expressions of type (1.9) and (1.10), which relate the model and real dimensionless numbers, were called the calibration relations. For the Prandtl number the calibration relation found in [25] can be represented by the equality

$$Pr_r = \left( \frac{1}{\gamma_0} + \frac{\gamma_0 - 1}{\gamma_0} \frac{1 + \varepsilon}{\varepsilon} \right) \frac{1}{\lambda} Pr \quad (1.15)$$

In a compressible stratified medium loss of stability of mechanical equilibrium occurs when  $Ra_r^S > Ra_r^{S*}$ , where  $Ra_r^{S*}$  is a threshold value. As mentioned above, in a near-critical fluid layer  $Ra_r^{S*} = 1708$  regardless of the proximity to the critical point. However, if we calculate the Rayleigh number for this medium neglecting stratification, convection will develop when  $Ra_r > Ra_r^*$ , where the threshold value  $Ra_r^*$  increases with the distance from the critical point. In what follows, these relations will be verified.

## 2. STABILITY THRESHOLD OF MECHANICAL EQUILIBRIUM

We will simulate Rayleigh-Bénard convection in  $^3\text{He}$  on the basis of experiments carried out in a cell 1 mm high and 57 mm in diameter under ground surface conditions [16]. On the upper and lower cell boundaries the temperature was maintained constant and increased very slowly, respectively. The average density was critical. In helium the critical point is reached when  $T'_c = 3.3189$  K,  $\rho'_c = 0.0414$  g/cm<sup>3</sup>, and  $P'_c = 0.117$  MPa [16]. The compressibility factor  $Z = 0.3074$ , where  $Z = P'_c/(B'\rho'_cT'_c)$ ,  $B' = R'/\mu'_g$ ,  $R' = 8.31 \cdot 10^7$  erg/(K·mole), and  $\mu'_g = 3$  g/mole.

In order to match the simulation parameters we need to know the experimental values of the Prandtl number  $\text{Pr}_e$  and the Rayleigh number divided by the temperature difference on the boundaries  $\text{Ra}_e/\Theta$ , which are calculated from the physical properties. In the critical neighborhood the properties of helium were determined on the interval  $5 \cdot 10^{-4} \leq \varepsilon \leq 0.2^1$ . The value of  $\text{Ra}_e/\Theta$  can be calculated from the expression

$$\frac{\text{Ra}_e}{\Theta} = \frac{T'_c \beta' g' l'^3 \rho'^2 c'_p}{\lambda' \eta'} = \frac{\beta c_p Z \text{Ra}}{\lambda \lambda_0 \Theta} \quad (2.1)$$

The specific heat  $c_p$  can be determined from  $c_v$  and  $\gamma$ :  $c_p = c_v \gamma$ . The coefficient  $\beta$  can be determined from the relation

$$\beta = \frac{c_v(\gamma - 1)}{(1 + \varepsilon)(\partial P/\partial T)_\rho} \quad (2.2)$$

which follows from (1.12) on nondimensionalization. In (2.1) and (2.2) the dimensionless quantities were obtained using the same scales as in [27]:  $P'_c/(\rho'_c T'_c)$  for  $c_p$  and  $c_v$ ,  $P'_c/T'_c$  for  $(\partial P/\partial T)_\rho$ ,  $1/T'_c$  for  $\beta$ , and  $\lambda'_0$  for  $\lambda$ . Professor H. Meyer has provided to us with a table of the experimental data on  $\lambda'$ ,  $c_v$ ,  $\gamma$ , and  $(\partial P/\partial T)_\rho$  and the values of  $\text{Pr}_e$ . The table also gives the values of  $\lambda$ ,  $c_p$ ,  $\beta$ , and  $\text{Ra}_e/\Theta$  calculated from these data. The model parameters can be determined from the experimental values on the basis of the conditions  $\text{Pr}_r = \text{Pr}_e$  and  $\text{Ra}_r/\Theta = \text{Ra}_e/\Theta$ , and then  $\text{Pr}$  and  $\text{Ra}/\Theta$  entering into the main system of equations can be calculated from (1.10) and (1.15). Below, we give the results of calculations for certain  $\varepsilon$ .

In view of the computational difficulties involved in carrying out the numerical calculations for a large-aspect ratio layer, in this simulation stage we considered a cell containing a single convective vortex in a 1 mm square domain. We assumed that the horizontal boundaries are isothermal with no-slip and the vertical boundaries adiabatic with slip. The system is characterized by the following dimensional and dimensionless quantities:

$$\begin{aligned} l' &= 0.1 \text{ cm}, \quad U' = 28.5 \text{ cm/s}, \quad g' = 9.8 \cdot 10^2 \text{ cm/s}^2, \quad \eta'_0 = 16.7 \cdot 10^{-6} \text{ g/(cm} \cdot \text{s)}, \\ c'_{v0} &= 4.12 \cdot 10^7 \text{ erg/(K} \cdot \text{g)}, \quad \lambda'_0 = 1.73 \cdot 10^{-4} \text{ W/cm} \cdot \text{K}, \quad \text{Re} = 8.33 \cdot 10^3, \\ \gamma &= 1.667, \quad \text{M} = 10^{-3}, \quad \Lambda = 0.0149, \quad \psi = 0.645 \end{aligned}$$

	$\varepsilon = 0.02, \text{Ra}/\theta = 2.271 \cdot 10^7, \text{Pr} = 1.056, \text{Ra}_r^* = 6190$				
$\text{Ra}_r$	6585	6545	6504	6464	6424
$\text{Nu}$	1.086	1.077	1.068	1.060	1.051
	$\varepsilon = 0.04, \text{Ra}/\theta = 1.842 \cdot 10^7, \text{Pr} = 0.9436, \text{Ra}_r^* = 2597$				
$\text{Ra}_r$	2721	2712	2703	2694	2684
$\text{Nu}$	1.064	1.059	1.054	1.050	1.045
	$\varepsilon = 0.06, \text{Ra}/\theta = 1.224 \cdot 10^7, \text{Pr} = 0.8528, \text{Ra}_r^* = 1902$				
$\text{Ra}_r$	1979	1973	1967	1961	1956
$\text{Nu}$	1.056	1.052	1.047	1.043	1.039
	$\varepsilon = 0.08, \text{Ra}/\theta = 1.121 \cdot 10^7, \text{Pr} = 0.8444, \text{Ra}_r^* = 1804$				
$\text{Ra}_r$	1915	1900	1884	1864	1853
$\text{Nu}$	1.082	1.071	1.059	1.048	1.034
	$\varepsilon = 0.10, \text{Ra}/\theta = 1.384 \cdot 10^7, \text{Pr} = 0.8145, \text{Ra}_r^* = 1804$				
$\text{Ra}_r$	1986	1961	1935	1908	1882
$\text{Nu}$	1.128	1.111	1.092	1.074	1.055

<sup>1</sup>H. Meyer. Table. Private communication.

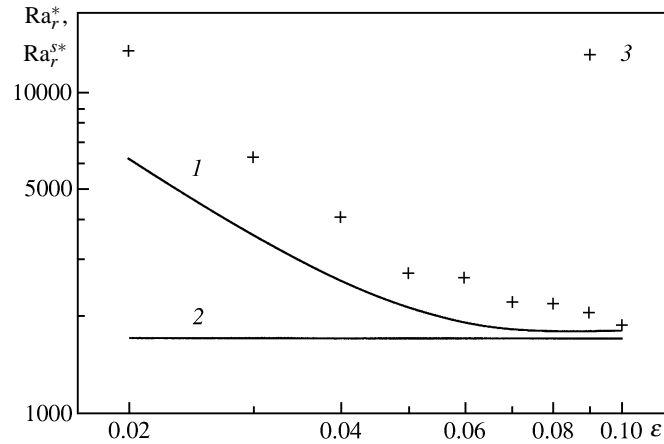


Fig. 1. Threshold Rayleigh numbers without and with allowance for stratification:  $Ra_r^*$  (curve 1) and  $Ra_r^{s*}$  (curve 2), and the experimental value  $Ra_r^{s*}$  [16] (3) as functions of the temperature parameter  $\epsilon$

The values of  $\lambda'_0$ ,  $\Lambda$ , and  $\psi$  were obtained in [22] by approximating the experimental data on the thermal conductivity (see footnote on page 214). The numerical method was described in [27].

We carried out five series of calculations for five values of the parameter  $\epsilon$  determined from the temperature of the upper boundary on the interval  $\epsilon \in [0.02-0.1]$ . In each series the temperature on the lower boundary was higher by a quantity  $\Theta$  than that on the upper boundary. This quantity was varied in different variants. We began to integrate the initial system of equations from the minimum value of  $\Theta$  and continued integrating until the fluid motion became steady-state. Then the lower surface was slowly heated to the next value of  $\Theta$  and the calculations were continued until another steady state was established. As a result, we obtained a series of steady-state solutions for various  $\Theta$ , each solution corresponding to its own value of  $Ra_r$ . In all the variants the Nusselt number  $Nu$  was determined from the expression

$$Nu = \frac{1}{j'} \int_0^{l'} \lambda' \frac{\partial T'}{\partial y'} dx', \quad j' = \lambda'_j \frac{\Theta'}{l'} \tag{2.3}$$

where  $j'$  and  $\lambda'_j$  are the heat flux and the thermal conductivity in the medium at rest. The  $Nu$  number characterizes the heat transfer rate in the presence of convection and can be calculated on the lower and upper boundaries; in steady-state flows the two quantities coincide. The values of  $Ra_r$  and  $Nu$  are given above. We used a  $61 \times 71$  vertically-nonuniform space grid, the time step was  $1 \cdot 10^{-4} - 3 \cdot 10^{-4}$ , the approach to the steady-state regime took  $3.5 \cdot 10^3$  s of physical time. The calculations were carried out using an AMD Athlon XP 1500 personal computer (1.33 GHz CPU frequency) and took approximately three months of computer time. For smaller  $\epsilon$  no calculations were carried out since they required too much computation time due to the deceleration of the relaxation processes the critical point is approached.

Using the solutions obtained, we determined the threshold number  $Ra_r^*$  for each  $\epsilon$ . For this purpose the dependences  $Nu$  at  $Ra_r$  were extrapolated to  $Nu = 1$  for which there is no convection; in the neighborhood of the stability threshold the functions  $Nu(Ra_r)$  were assumed to be linear. Above, we have presented the  $Ra_r^*$  numbers which, as can be seen, increase with decrease in  $\epsilon$ . In Fig. 1 we have plotted graphs of the function  $Ra_r^*(\epsilon)$  and compared it with the experimental data [16]. We note that the results of the calculations for  $\epsilon \sim 0.1$  are in fairly good agreement with the experimental data, but as  $\epsilon$  decreases the agreement becomes only qualitative. A similar quantitative discrepancy is attributable to using the Van-der-Waals equation of state which, as is well known, describes the near-critical fluid with low accuracy. The growth in  $Ra_r^*$  with increase in the compressibility of the medium was also detected in the case of a perfect gas [10].

Then for each  $Ra_r$  we calculated  $Ra_r^s$  from (1.9), (1.14) with allowance for stratification. In Fig. 2 we have reproduced graphs of the function  $Nu(Ra_r^s)$  for various  $\epsilon$ . When  $\epsilon \geq 0.06$  the role of the compression effects

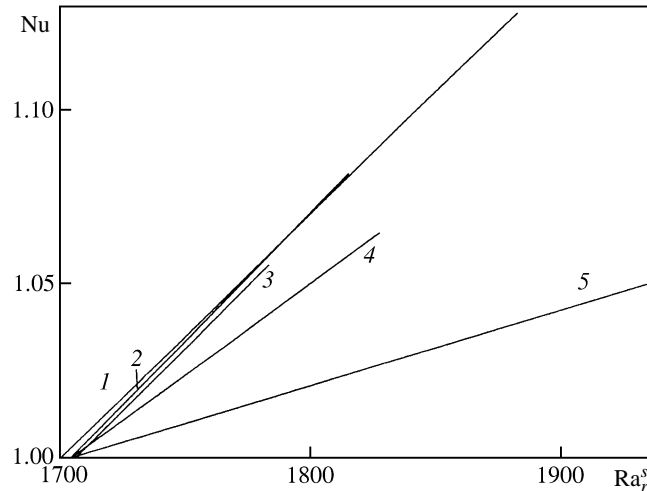


Fig. 2. Nusselt number  $Nu$  as a function of the Rayleigh number  $Ra_r^s$  for  $\varepsilon = 0.1, 0.08, 0.06, 0.04,$  and  $0.02$  (curves 1–5, respectively)

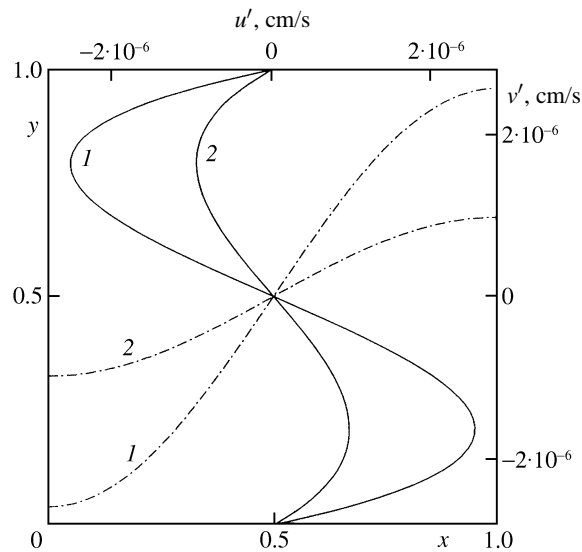


Fig. 3. Distributions of the horizontal  $u'(0.5, y)$  (continuous curves) and vertical  $v'(x, 0.5)$  (chain curves) velocity components for  $\varepsilon = 0.1$  and  $0.02$  (curves 1 and 2, respectively)

is insignificant and the straight lines almost coincide. However, when  $\varepsilon < 0.06$  the angle of inclination of the straight lines becomes smaller, i.e., the increase in the Nusselt number slows as the distance from the critical point decreases. The heat transfer beyond the stability threshold will be analyzed in the next section. Similar behavior of the Nusselt number with increase in the compressibility of the medium was also observed in a perfect gas [11].

Using  $Nu(Ra_r^s)$ , we calculated the threshold values of  $Ra_r^{s*}$  reached at  $Nu = 1$ ; they are presented in Fig. 1. They show that the value of  $Ra_r^{s*}$  is almost constant for all  $\varepsilon$ ; the maximum deviation from  $Ra_r^{s*} = 1708$  is not more than 0.5%.

### 3. COMPRESSIBILITY EFFECTS IN STEADY-STATE FLOWS

In what follows we will compare two flows which develop in media of different compressibilities (for  $\varepsilon = 0.1$  and  $\varepsilon = 0.02$ ) but create heat transfer with the same Nusselt number:  $Nu = 1.051$ . As follows from Fig. 2, the compression effects are small in the first case and significant in the second.

Figure 3 illustrates the distributions of the horizontal and vertical velocity components  $u'(0.5, y)$  and

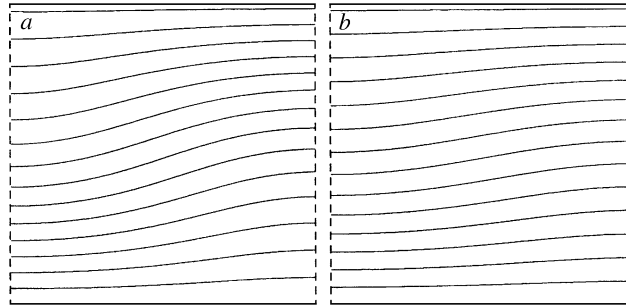


Fig. 4. Isotherms for  $\varepsilon = 0.1$  (a) and  $\varepsilon = 0.02$  (b)

$v'(x, 0.5)$  along the central vertical and horizontal lines and shows that the flow velocity decreases with decrease in  $\varepsilon$ . Accordingly, for  $\varepsilon = 0.02$  the thermal field turns out to be more uniform than for  $\varepsilon = 0.1$ , i.e., in the first case the isotherms represented in Fig. 4 are less curved. Thus, with decrease in  $\varepsilon$  the intensification of heat transfer characterized by the same value of Nu takes place in the less intense flow. This means that in addition to convection a further mechanism, which creates an additional temperature gradient in the neighborhood of the boundary, appears with increase in compressibility.

The nature of this mechanism is related to the thermodynamics of the medium whose state can generally be described by the relation

$$dT' = -\frac{1}{\rho'\beta'}d\rho' + \left(\frac{\partial T'}{\partial P'}\right)_{\rho'} dP' \quad (3.1)$$

In weakly compressible media the second term on the right side is much less than the first; therefore, the variations of the temperature are determined only by the variations of the density, i.e., in the presence of heat inflow due to heat conduction and internal friction, the density decreases owing to thermal expansion, while the temperature increases. When the parameters of the medium tend to the critical values and the thermal expansion coefficient  $\beta'$  tends to infinity, the first term on the right tends to zero and becomes commensurable with the second. Under these conditions effects driven by the pressure difference begin to manifest themselves.

In the gravity force field the pressure increases downwards. If a fluid element rises, it is subjected to steadily lower pressure from the surrounding mass; therefore, it expands and cools. Conversely, the pressure on a descending volume element increases, compressing and heating it. Thus, an additional temperature gradient associated with adiabatic compression of the medium and directed downward appears in the presence of stratification. In absolute value this temperature gradient coincides with the adiabatic temperature gradient  $(\partial\Theta'/\partial y')_{ad}$  since, like the latter, it is formed under isentropic conditions in the stratified medium. The formation of an adiabatic temperature gradient was confirmed experimentally in [16].

In Fig. 5 we have plotted graphs of the density, pressure, and temperature as functions of the height at the center of a computation cell. Clearly, as compared with  $\varepsilon = 0.10$ , in the flow with  $\varepsilon = 0.02$  the density drops  $\Delta\rho' = \rho' - \rho'_c$  are reduced by several times (Fig. 5a) and, in accordance with Table 1, the coefficient  $\beta'$  increases by 6.4 times; therefore, in fact, the first term in (3.1) sharply decreases. The pressure function  $p'$  varies only slightly (Fig. 5b) so that the second term in (3.2) also varies only slightly and makes a weightier contribution to the temperature increment. In Fig. 5b we have reproduced the dynamic pressure  $p'$  whose gradient coincides with the total pressure gradient  $P'$  since the average value  $\langle P' \rangle = P' - p'$  is independent of the space coordinates. As the distance from the critical point decreases, the temperature difference  $\Delta T' = T' - T'_i$  determining the motion is reduced due to the increase in  $\beta'$  (Fig. 5b). This was detected experimentally in [16]. The convection flow smoothes the stratification inhomogeneities leading to a more uniform vertical mass distribution: when  $\varepsilon = 0.02$  the density drops  $\Delta\rho'$  in the moving fluid turn out to be less than those under equilibrium conditions  $\Delta\rho'_e = \rho'_e - \rho'_c$  (Fig. 5a).

Thus, an additional temperature gradient develops in the stratified compressible medium. This gradient is not related with heat transfer but enters into the Nusselt number calculations (2.3). In order to determine

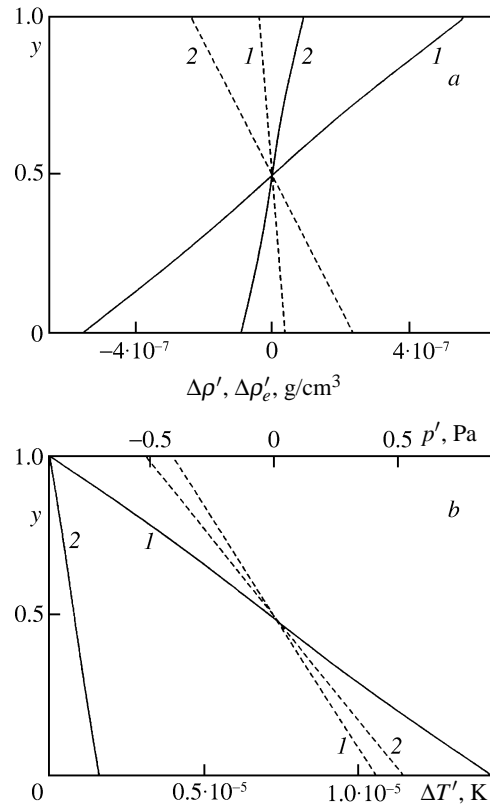


Fig. 5. Deviation of the density from the critical density during motion  $\Delta\rho'$  (continuous curves) and under conditions of mechanical equilibrium (broken curves) (a) and deviation of the temperature from the initial temperature  $\Delta T'$  (continuous curves) and the dynamic pressure (broken curves) (b) in the central vertical cross-section for  $\varepsilon = 0.1$  and  $0.02$  (curves 1 and 2, respectively)

how much the convection flow really intensifies the heat transfer as compared with heat conduction it is necessary to consider the modified Nusselt number  $Nu_s$ , excluding the adiabatic temperature gradient:

$$Nu_s = \frac{1}{j'_s} \int_0^{l'} \lambda' \left( \frac{\partial T'}{\partial y'} - \left( \frac{\partial \Theta'}{\partial y'} \right)_{ad} \right) dx', \quad j'_s = \lambda'_j \left( \frac{\Theta'}{l'} - \left( \frac{\partial \Theta'}{\partial y'} \right)_{ad} \right) \quad (3.2)$$

Under the conditions investigated  $\Theta \ll \varepsilon$ ; therefore, the physical properties of the near-critical fluid vary only slightly over space. This makes it possible to assume that in the medium at rest  $\Theta'/l' = \partial\Theta'/\partial y'$  and in the presence of convection  $\lambda' = \lambda'_j$  and reduce the expression for  $Nu_s$  to the form:

$$Nu_s = 1 + (Nu - 1) \frac{1}{k} \quad (3.3)$$

The coefficient  $k$  was defined in (1.9).

We calculated  $Nu_s$  for all the available values of  $Nu(Ra_r^s)$  and the results are shown in Fig. 6. For comparison purposes we have also reproduced the dependence obtained from the experimental data for air which on the interval  $1708 < Ra < 5830$  has the form [28]:

$$Nu = 1 + 1.44 \left( 1 - \frac{1708}{Ra} \right) \quad (3.4)$$

The experiments were carried out under ordinary conditions far from the critical point, and the air was only slightly compressible so that  $Ra_r^s = Ra$  and  $Nu_s = Nu$ . The calculated points fit the experimental curve

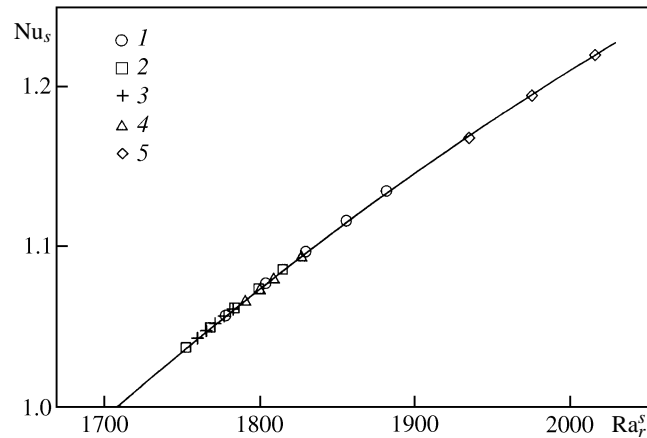


Fig. 6. Nusselt number  $Nu_s$  as a function of the Rayleigh number  $Ra_r^s$  in the calculations carried out in the present study for  $\varepsilon = 0.1, 0.08, 0.06, 0.04,$  and  $0.02$  (curves 1–5, respectively) and obtained experimentally [28] (continuous curve)

with high accuracy, i.e., convection in a highly compressible near-critical fluid intensifies the heat transfer on the boundary in the same way as in a weakly compressible medium.

*Summary.* In order to determine the stability threshold of mechanical equilibrium of a near-critical fluid in the Rayleigh-Bénard problem it is necessary to know the real dimensionless numbers, in particular, the Rayleigh number. The numerical simulation carried out using experimental data for near-critical helium [16] showed that the threshold value  $Ra_r^*$  calculated without allowance for stratification increases as the distance to the critical point decreases. The agreement between this result and the experimental data is qualitative, evidently due to the use of an insufficiently exact equation of state. However, by using this approach, on the basis of the experimental dependence for the threshold values  $Ra_r^*$  we can choose an equation of state which describes the medium more accurately in the neighborhood of the critical point.

For a stratified medium a calibration relation is found for the real Rayleigh number  $Ra_r^s$ . The threshold value  $Ra_r^*$  calculated in the study is almost constant regardless of the proximity to the critical point. This result is in complete agreement with theory [13] and experiment [16]. This confirms the validity of the calibration relation obtained for  $Ra_r^s$  and the technique for determining the model parameters from the experimental data.

When a compressible medium moves, in the case of steady-state convection flows beyond the stability threshold an additional temperature gradient equal to the adiabatic temperature gradient is formed. This temperature gradient is not related with the heat transfer but is due to the pressure gradient. In order to determine the convective heat transfer this temperature gradient must be eliminated from the calculations for the Nusselt number. The Nusselt number thus calculated indicates that convective heat transfer in highly and weakly compressible media has the same intensity. Earlier, adiabatic compression effects were detected in the time-dependent flows of a near-critical fluid. In particular, the piston effect in which the medium is heated while being compressed under the action of the boundary layer pressure is well known. In the present study the adiabatic compression effect manifested in steady-state flows is investigated.

The authors wish to thank Professor H. Meyer for the data on physical properties of helium in the neighborhood of the critical point.

The work was carried out with financial support from the Russian Foundation for Basic Research (projects Nos. 03-01-00682 and 04-01-00630).

## REFERENCES

1. E. L. Kosechmieder, *Bénard Cells and Taylor Vortices*, Cambridge Univ. Press, Cambridge (1993).
2. A. V. Getling, *Rayleigh-Bénard Convection. Structures and Dynamics* [in Russian], Editorial URSS, Moscow (1999).

3. E. Bodenschatz, W. Pesch, and G. Ahlers, "Recent developments in Rayleigh-Bénard convection," *Annu. Rev. Fluid Mech.*, **32**, 709 (2000).
4. V. I. Polezhaev and V. P. Yaremchuk, "Numerical simulation of unsteady two-dimensional convection in a finite-length horizontal layer heated from below," *Fluid Dynamics*, **36**, No. 4, 556 (2001).
5. M. K. Ermakov, M. N. Myakshina, S. A. Nikitin, and V. P. Yaremchuk, "Computer laboratory and computer practical work on convective heat and mass transfer," in: *3rd Russ. Nat. Conf. on Heat Transfer*, Vol. 3 [in Russian], Moscow Energy Institute Press, Moscow (2002), P. 72–75.
6. M. A. Anisimov, *Critical Phenomena in Liquids and Liquid Crystals* [in Russian], Nauka, Moscow (1987).
7. L. D. Landau and E. M. Lifshitz, *Theoretical Physics. Vol. 6. Hydrodynamics* [in Russian], Nauka, Moscow (1986).
8. V. I. Polezhaev, A. A. Gorbunov, and E. B. Soboleva, "Classical problems of convection near critical point," *Adv. Space Res.*, **29**, 581 (2002).
9. H. Jeffreys, "The stability of a compressible fluid heated from below," *Proc. Camb. Phil. Soc.*, **26**, 170 (1930).
10. V. I. Polezhaev, "Flow and heat transfer with natural convection of a gas in a closed region after loss of hydrostatic equilibrium stability," *Fluid Dynamics*, **3**, No. 5, 82–85 (1968).
11. V. I. Polezhaev and M. P. Vlasyuk, "On cell convection in an infinite horizontal gas layer heated from below," *Dokl. Akad. Nauk SSSR*, **195**, No. 5, 1058 (1970).
12. M. Sh. Giterman and V. A. Shteinberg, "Criteria of onset of convection in a fluid in the neighborhood of the critical point," *Teplofizika Vysokikh Temperatur*, **8**, 799 (1970).
13. P. Carlès and B. Ugurtas, "The onset of free convection near the liquid-vapor critical point. P. I: Stationary initial state," *Physica D*, **126**, 69 (1999).
14. T. Maekawa and K. Ishu, "Temperature propagation and convective instabilities in critical fluid," in: *Proc. Conf. Fundamental Physics and Chemical Physics under Microgravity*, NASDA Conf. Publications, CON-000003E (2000), P. 27–30.
15. M. Assenheimer and V. Steinberg, "Rayleigh-Bénard convection near the gas-liquid critical point," *Phys. Rev. Lett.*, **70**, No. 25, 3888 (1993).
16. A. B. Kogan and H. Meyer, "Heat transfer and convection onset in a compressible fluid:  $^3\text{He}$  near the critical point," *Phys. Rev. E*, **63**, No. 5, Paper 056310 (2001).
17. S. Amiroudine, P. Bontoux, P. Laroude, B. Gilly, B. Zappoli, "Direct numerical simulation of instabilities in a two-dimensional near-critical fluid layer heated from below," *J. Fluid Mech.*, **442**, 119 (2001).
18. A. Furukava and A. Onuki, "Convective heat transport in compressible fluids," *Phys. Rev. E*, **66**, No. 1, Paper 016302 (2002).
19. P. Carlès and L. El Khouri, "Scenarios for the onset of convection close to the critical point," *Phys. Rev. E*, **66**, No. 6, Paper 066309 (2002).
20. S. Amiroudine and B. Zappoli, "Piston-effect-induced thermal oscillations at the Rayleigh-Bénard threshold in supercritical  $^3\text{He}$ ," *Phys. Rev. Lett.*, **90**, No. 10, Paper 105303 (2003).
21. A. Onuki, H. Hao, and R. A. Ferrell, "Fast adiabatic equilibrium in a single-component fluid near the liquid-vapor critical point," *Phys. Rev. A*, **41**, No. 4, 2256 (1990).
22. V. I. Polezhaev and E. B. Soboleva, "Thermal gravity-driven convection of near-critical helium in enclosures," *Low Temperature Physics*, **29**, 484 (2003).
23. V. I. Polezhaev and E. B. Soboleva, "Unsteady thermo-gravitational convection effects in a side-heated or cooled near-critical fluid," *Fluid Dynamics*, **37**, No. 1, 72 (2002).
24. A. G. Churbanov, A. N. Pavlov, A. V. Voronkov, and A. A. Ionkin, "Prediction of low Mach number flows: a comparison of pressure-based algorithms," in: *Proc. 10th Intern. Conf. Swansea, U.K.*, Vol. 10 (1997), P. 1099.
25. V. I. Polezhaev and E. B. Soboleva, "Thermo-gravitational convection in a near-critical fluid in a side-heated enclosed cavity," *Fluid Dynamics*, **36**, No. 3, 467 (2001).
26. L. D. Landau and E. M. Lifshitz, *Theoretical Physics. Vol. 5. Statistical Physics* [in Russian], Nauka, Moscow (1976).
27. E. B. Soboleva, "Adiabatic heating and convection caused by a fixed-heat-flux source in a near-critical fluid," *Phys. Rev. E*, **68**, No. 4, Paper 042201 (2003).
28. J. Jaluria, *Natural Convection*, Pergamon Press, Oxford (1980).